Title

Application of a glycinated bile acid biomarker for diagnosis and assessment of response to treatment in Niemann-pick disease type C1

Journal

Molecular Genetics and Metabolism, 131(4)

ISSN

1096-7192

Authors

Sidhu, Rohini
Kell, Pamela
Dietzen, Dennis J
et al.

Publication Date

2020-12-01

DOI

10.1016/j.ymgme.2020.11.005

Peer reviewed

HHS Public Access

Author manuscript

Mol Genet Metab. Author manuscript; available in PMC 2021 December 01.

Published in final edited form as:

Mol Genet Metab. 2020 December ; 131(4): 405–417. doi:10.1016/j.ymgme.2020.11.005.

Application of a Glycinated Bile Acid Biomarker for Diagnosis and Assessment of Response to Treatment in Niemann-Pick Disease Type C1

Rohini Sidhu[1,$], **Pamela Kell**[1], **Dennis J. Dietzen**[4], **Nicole Y. Farhat**[5], **An Ngoc Dang Do**[5], **Forbes D. Porter**[5], **Elizabeth Berry-Kravis**[6], **Janine Reunert**[7], **Thorsten Marquardt**[7], **Roberto Giugliani**[8], **Charles M. Lourenço**[9], **Raymond Y. Wang**[10,11], **Nina Movsesyan**[12], **Ellen Plummer**[13], **Jean E. Schaffer**[1,#], **Daniel S. Ory**[1,$], **Xuntian Jiang**[1,*]

[1]Department of Medicine, Washington University School of Medicine, St. Louis, MO 63110, USA

[4]Department of Pathology & Immunology, Washington University School of Medicine, St. Louis, MO 63110, USA

[5]Section on Molecular Dysmorphology, *Eunice Kennedy Shriver* National Institute of Child Health and Human Development, NIH, DHHS, Bethesda, MD 20892, USA

[6]Rush University Medical Center, Chicago, IL 60612, USA

[7]Klinik und Poliklinik für Kinder- und Jugendmedizin - Allgemeine Pädiatrie, Universitätsklinikum Münster, Albert-Schweitzer-Campus 1, Gebäude A1, 48149, Münster, Germany

[8]Department of Genetics, UFRGS, Medical Genetics Service, HCPA, BioDiscovery Laboratory, HCPA, Hospital de Clínicas de Porto Alegre, and National Institute of Population Medical Genetics - INAGEMP, Porto Alegre RS 90035-903, Brazil

[9]Faculdade de Medicina - Centro Universitario Estácio de Ribeirão Preto, Rua Abrahão Issa Halach, 980 – Ribeirânia, Ribeirão Preto – SP, Brazil

[10]Division of Metabolic Disorders, CHOC Children's Specialists, Orange, CA 92868, USA

[11]Department of Pediatrics, University of California-Irvine School of Medicine, Orange, CA 92868, USA

[12]Research Institute, CHOC Children's Hospital, Orange, CA 92868, USA

[13]Asante Pediatric Hematology and Oncology - Medford, Medford, OR, 97504, USA.

Abstract

Niemann-Pick disease type C (NPC) is a neurodegenerative disease in which mutation of *NPC1* or *NPC2* gene leads to lysosomal accumulation of unesterified cholesterol and sphingolipids.

[*]To whom correspondence should be addressed: Xuntian Jiang, PhD, jiangxuntian@wustl.edu.
[#]:Current address: Joslin Diabetes Center, Harvard Medical School, Boston, MA 02115, USA
[$]:Current address: Casma Therapeutics, Cambridge, MA 02139, USA

Diagnosis of NPC disease is challenging due to non-specific early symptoms. Biomarker and genetic tests are used as first-line diagnostic tests for NPC. In this study, we developed a plasma test based on N-(3β,5α,6β-trihydroxy-cholan-24-oyl)glycine (TCG) that was markedly increased in the plasma of human NPC1 subjects. The test showed sensitivity of 0.9945 and specificity of 0.9982 to differentiate individuals with NPC1 from NPC1 carriers and controls. Compared to other commonly used biomarkers, cholestane-3β,5α,6β-triol (C-triol) and N-palmitoyl-O-phosphocholine (PPCS, also referred to as lysoSM-509), TCG was equally sensitive for identifying NPC1 but more specific. Unlike C-triol and PPCS, TCG showed excellent stability and no spurious generation of marker in the sample preparation or aging of samples. TCG was also elevated in lysosomal acid lipase deficiency (LALD) and acid sphingomyelinase deficiency (ASMD). Plasma TCG was significantly reduced after intravenous (IV) 2-hydroxypropyl-β-cyclodextrin (HPβCD) treatment. These results demonstrate that plasma TCG was superior to C-triol and PPCS as NPC1 diagnostic biomarker and was able to evaluate the peripheral treatment efficacy of IV HPβCD treatment.

Keywords

Bile acid; N-(3β,5α,6β-trihydroxy-cholan-24-oyl)glycine; Niemann-Pick disease type C; diagnosis; 2-hydroxypropyl-β-cyclodextrin; treatment assessment

INTRODUCTION

Niemann-Pick disease type C (NPC) is a rare neurovisceral lysosomal storage disorder caused by defects in the cholesterol trafficking NPC1 (95% cases) (1) or NPC2 (5% cases) (2) proteins, resulting in lysosomal accumulation of unesterified cholesterol and sphingolipids (3). The varying onset and early non-specific symptoms of NPC disease contribute to the difficulty in diagnosis of the disorder (4). The current diagnostic approach includes both biomarker profiling and genetic analysis (5, 6). Filipin staining, the historical gold standard assay for NPC diagnosis, is used to confirm a diagnosis in patients for whom inconclusive genetic testing and blood biomarker results are obtained (6).

The most well validated NPC plasma diagnostic biomarkers include oxysterols (5, 7-22), N-palmitoyl-O-phosphocholine (PPCS, also referred to as lysoSM-509) (21, 23-29), and bile acids (30, 31). Clinically, oxysterols are the most widely used biomarkers for NPC diagnostics (7, 8). The oxysterol biomarkers include cholestane-3β,5α,6β-triol (C-triol), which has been shown by numerous major clinical laboratories to be a robust and sensitive biomarker for NPC (5, 7, 9-15, 17-20, 22). PPCS was first reported by Rolfs group (23) and used for NPC diagnosis even though its molecular identity was unknown (20, 21, 23-28). Recently, the structure of this novel lipid was identified (32) and a clinical grade assay using authentic standard compound was developed (29). Diagnostics based on (3β,5α,6β-trihydroxy-cholan-24-oyl)glycine (TCG), the most specific bile acid biomarker, has been in the clinic for more than 3 years and a TCG-based newborn screening assay for NPC1 is currently being piloted (30, 33). Here, we report the plasma TCG test for NPC1 diagnosis and compare its sensitivity and specificity with C-triol and PPCS. We also utilized TCG to assess treatment efficacy following interventions with miglustat or intrathecal (IT) (34-37)

and intravenous (IV) (38, 39) 2-hydroxypropyl-β-cyclodextrin (HPβCD) administration to treat central nervous system and visceral manifestations of the disease, respectively.

MATERIALS AND METHODS

Chemicals and reagents

The 3-[(3-cholamidopropyl)dimethylammonio]-1-propanesulfonate (CHAPS) was obtained from VWR (West Chester, PA). The sodium dodecyl sulfate (SDS), sodium hydroxide, diethylamine, and hexafluoro-2-propanol were purchased from Sigma (St. Louis, MO). The high performance liquid chromatography (HPLC) grade methanol and acetonitrile were purchased from EMD Chemicals (Gibbstown, NJ). Milli-Q ultrapure water was prepared in-house with a Milli-Q Integral Water Purification System (Billerica, MA). Pooled human plasma was purchased from Biochemed (Winchester, VA).

Clinical studies

Human studies adhered to the principles of the Declaration of Helsinki, as well as to Title 45, US Code of Federal Regulations, Part 46, Protection of Human Subjects. Informed consent was obtained from the participants or their guardians. Assent was obtained when applicable. The clinical protocols were approved by the Institutional Review Boards of NICHD/NIH, Rush University Medical Center (RUMC), Universitätsklinikum Münster, Hospital de Clínicas de Porto Alegre, Centro Universitario Estácio de Ribeirão Preto, Washington University School of Medicine, Asante Pediatric Hematology and Oncology – Medford, and Children's Hospital of Orange County. All the clinical samples were de-identified, and the analysis of de-identified human samples was approved by the Human Studies Committee at Washington University.

Collection of plasma samples for diagnostic assay development

All plasma samples were collected in ethylenediamine tetraacetic acid dipotassium salt containing tubes. The NPC1 and NPC1 carrier plasma samples were collected from affected and obligate heterozygote study participants, respectively, at NICHD/NIH, RUMC, Universitätsklinikum Münster, and Centro Universitario Estácio de Ribeirão Preto. The longitudinal natural history study of NPC disease was conducted at NIH. NIH also provided plasma samples from study participants with familial hypercholesterolemia (FH, mutations in *LDLR, APOB*, and *PCSK9* genes), and Batten disease resulting from mutations in *CLN3*. Hospital de Clínicas de Porto Alegre collected plasma samples from patients affected with mucopolysaccharidosis (MPS) type I (mutations in *IDUA* gene), II (mutations in *IDS* gene), IIIA (mutations in *SGSH* gene), IIIB (mutations in *NAGLU* gene), IIIC (mutations in *HGSNAT* gene), IVA (mutations in *GALNS* gene), VI (mutations in *ARSB* gene), VII (mutations in *GUSB* gene), GM1 gangliosidosis (GM1, mutations in *GLB1* gene), GM2 gangliosidosis (GM2) including Tay-Sachs (mutations in *HEXA* gene) and Sandhoff (mutations in *HEXB* gene), Batten disease resulting from mutations in *CLN1* and *CLN2* genes, mucolipidosis (ML) type II/III (mutations in *GNPTAB* gene), Fabry (mutations in *GLA* gene), Krabbe (mutations in *GALC* gene), and Gaucher diseases (mutations in *GBA* gene). Centro Universitario Estácio de Ribeirão Preto also provided plasma samples from individuals affected with acid-sphingomyelinase deficiency (ASMD, mutations in *SMPD1*

gene), Wolman (mutations in *LIPA* gene), Tay-Sachs, cerebrotendinous xanthomathosis (CTX, mutations in *CYP27A1* gene), Fabry, and spastic paraplegia type 5 (SPG5, mutations in *CYP7B1* gene). Universitätsklinikum Münster collected plasma samples from individuals affected with ASMD and cholesteryl ester storage disease (CESD, mutations in *LIPA* gene), and ASMD carriers. Residual de-identified plasma samples were obtained from the Washington University Metabolomics Core. Age appropriate control plasma samples were obtained from anonymized residual samples at St. Louis Children's Hospital.

Collection of plasma samples from IT HPβCD treatment of NPC disease

The Phase 1/2a open-label, dose-escalation study of monthly intrathecal doses of 50 - 1200 mg of HPβCD was performed at NIH and open-label expanded access protocol with every two weekly intrathecal doses of 200-1200 mg HPβCD was performed at RUMC, and the detailed protocols were described in recent papers (35, 37). The patients CDA101 - 114 have received 11 - 29 infusions at monthly visits to NIH, and the patients Rush001 - 004 have received 5 - 39 infusions at biweekly visits to RUMC. The dosing diagram is given in the Figure 1. The plasma samples were collected from prior to the timed doses. The samples collected at baseline visit were pre-treatment samples.

Collection of plasma samples from IV HPβCD treatment of NPC disease

Under FDA-approved individual patient investigational new drug applications, two female NPC1 patients (patients 1 and 2) and a male NPC1 patient started IV HPβCD at 21 months, 10 years, and 13 years old, respectively. The doses for patients 1, 2, and 3 were 500, 2000, and 2000 mg/kg/week, respectively. The plasma samples were collected before administration of HPβCD from patient 1 at Children's Hospital of Orange County, and from patients 2 and 3 at Asante Pediatric Hematology and Oncology - Medford.

Stock solution preparation

All the stock solutions (1 mg/mL) were prepared in acetonitrile-water (1:1). The internal standard working solution for human plasma (20 ng/mL of [$^{13}C_2$, ^{15}N]-TCG) was prepared in water containing SDS (1%) and sodium hydroxide (1M).

Standard curves

Because of the presence of endogenous TCG in plasma, 2% CHAPS aqueous solution was used to prepare the calibration standards. Calibration curves were prepared by spiking TCG stock solution into 2% CHAPS solution, and preparing serial dilutions that yielded eight-point calibration standards for human plasma (1 - 1000 ng/mL of TCG). 2% CHAPS solution served as blank. The same calibration standards in human plasma were also prepared and used to assess responsiveness in different matrixes, which was evaluated by parallelism between standard curves prepared in biological matrix (human plasma) and surrogate matrix (2% CHAPS solution).

Quality control samples

The quality control (QC) samples were prepared by spiking TCG into pooled control human plasma, of which the mean concentration (n = 12) of endogenous TCG was determined by

the LC-MS/MS method. The pooled control human plasma was served as lower limit QC (LLQC), as endogenous TCG level (1.67 ng/mL) was close to lower limit of quantification (LLOQ, 1 ng/mL). The low (LQC, endogenous level + 10 ng/mL), middle (MQC, endogenous level + 400 ng/mL), high (HQC, endogenous level + 800 ng/mL), dilution (DQC, endogenous level + 1600 ng/mL) quality control samples were prepared for human plasma. The LLOQ samples for plasma (1 ng/mL) was prepared in 2% CHAPS solution. TCG concentrations in DQC samplers were higher than the upper limit of quantification (ULOQ: 1000 ng/mL). DQC samples were diluted 1:4 with 2% CHAPS solution, prior to extraction.

Effect of hemolysis

To evaluate the effect of hemolysis, the hemolyzed plasma with hemoglobin concentrations (0, 200, 400, 600, 800 mg/dL) was prepared by mixing a second lot of control plasma with lysed human red blood cells. The hemolyzed LQC (H-LQC, endogenous level + 1 ng/mL) and HQC (H-HQC, endogenous level + 80 ng/mL) samples were prepared in hemolyzed plasma.

Sample preparation

Standards, QCs, blank, and study samples (50 μL) were aliquoted into 96-well (1 mL/well) plate (Analytical Sales and Services, Flanders, NJ). Internal standard working solution (50 μL) was added except that aqueous 1% SDS (1%) and sodium hydroxide (1M) (50 μL) solution was used for a blank, followed by addition of acetonitrile (300 μL). The samples were vortexed for approximately 3 minutes and then centrifuged at 3,750 rpm for 10 minutes. Supernatants (300 μL) were transferred to a new 96-well (1 mL/well) plate, dried with nitrogen flow at 50 °C, and reconstituted in water (150 μL).

LC-MS/MS analysis

LC–MS/MS analysis was conducted on a Shimadzu (Columbia, MD) Prominence HPLC system coupled with an Applied Biosystems/MDS Sciex (Ontario, Canada) 4000QTRAP mass spectrometer using positive multiple reaction monitoring (MRM). The ESI source temperature was 550 °C; the ESI needle was −4500 V; the declustering potential was - 140 V; the entrance potential and the collision cell exit potential were −10 and −11 V, respectively. The collision and curtain gas were set at medium and 20, respectively. The desolvation gas and nebulizing gas were set at 60 and 30, respectively. For MRM, the collision energies for mass transitions of both *m/z* 464.3 to 74 (TCG) and *m/z* 467.3 to 77 ([$^{13}C_2$, ^{15}N]-TCG) was −72 eV. The dwell time was set at 200 and 50 ms for TCG and [$^{13}C_2$, ^{15}N]-TCG), respectively.

The HPLC system consists of Prominence HPLC system with a CBM-20A system controller, 2 LC-20AD pumps, a SIL-20ACHT autosampler, and a DGU-20A5R degasser. The chromatography was performed at ambient temperature using ACE Excel 3 Super C18 (4.6 x 100 mm, 3 μm, MAC-MOD Analytical, Chadds Ford, PA) protected with a Gemini C18 Securityguard™ column (4 x 3.0 mm, Phenomenex, Torrance, CA). The compartment of the autosampler was set at 4 °C. The mobile phases A (2.9 mM diethylamine and 20 mM hexafluoro-2-propanol in water) and B (acetonitrile-methanol (1:4)) were used in the

gradient elution. The gradient elution at a flow rate of 1 ml/min was started at 45% B, linearly increased from 45% to 55% in 3.5 min, and then increased from 55% to 100% in 0.1 min, where it was held for 1.4 min. The gradient was then returned to initial conditions in 0.1 min, where it was held for 1.9 min before the next injection, for a total run time of 7 min. The LC flow was diverted to waste except for 3.5 −4.5 min to mass spectrometer. Injection volume was 20 μL. Data were acquired and analyzed by Analyst software (version 1.5.2). Calibration curves were constructed by plotting the corresponding peak area ratios of analyte/intemal standard versus the corresponding analyte concentrations using weighted ($1/x^2$) least squares regression analysis.

Validation of linearity, precision and accuracy

The linearity, precision and accuracy of assay were evaluated over three analytical runs (40). In the validation analytical run, a set of samples that were analyzed in one batch, including calibration standards in duplicate, a blank, a blank with internal standard, and QC samples. This set of samples were prepared and analyzed in three different batches. The replication was the repeated preparation and analysis of the same sample. The linearity response of TCG was assessed over 1 - 1000 ng/mL. The precision and accuracy of the assay were determined for TCG in plasma at LLOQ, LLQC, LQC, MQC and HQC levels. For each QC concentration, analysis was performed in six replicates on each day except for DQCs for which three replicates were prepared in the first batch. H-LQC and H-HQC samples were analyzed in three replicates. Accuracy and precision were denoted by percent relative error (%RE) and percent coefficient of variance (%CV), respectively. The accuracy and precision were required to be within ± 15% RE of the nominal concentration and ≤15% CV, respectively, for LLQC, LQC, MQC, HQC, DQC, H-LQC, and H-HQC samples. The accuracy and precision were required to be within ± 20% RE of the nominal concentration and ≤20% CV for LLOQ samples in the intra-batch and inter-batch assays.

Sample stability

The long-term storage, freeze/thaw stabilities, and stabilities on the bench-top and in the autosampler were determined at the LQC and HQC concentration levels (n = 3). Long-term storage stability of TCG in plasma was tested up to 448 days upon storage at −80 °C. Bench-top stability was evaluated from plasma that was kept on lab bench at room temperature for 24 hours before sample extraction. Freeze/thaw stability was tested by freezing the plasma samples at −80 °C overnight, followed by thawing to room temperature the next day. This process was repeated five times. In the autosampler, stability at 4 °C was tested over 4 days by injecting the first batch of the validation samples. The whole blood stability was tested by analysis of a whole blood from a control subject after storage at 4 °C and room temperature for 18 hours. Stock solution stability was established by quantification of samples from dilution of two stock solutions that were stored at −20 °C for 448 days and at room temperature on the bench for 24 hours, respectively, to the final solution (1000 ng/mL in acetonitrile-water (1:1)). A fresh standard curve was established each time.

Analysis of human plasma samples

Samples consisted of calibration standards in duplicate, a blank, a blank with internal standard, QC samples (LQC, MQC and HQC), and unknown clinical samples were

analyzed. The standard curve covered the expected unknown sample concentration range, and samples that exceeded the highest standard were diluted and re-assayed. In the dilution sample re-assay, a diluted QC in triplicate would be also included in the analytical run. The results of the QC samples provided the basis of accepting or rejecting the run according to FDA guidelines (40). The endogenous TCG levels below the LLOQ (1 ng/mL) were reported as "< 1 ng/mL".

Statistics

For group comparisons, and the statistical significance of differences in mean values was determined by a two-tailed Student's t test and one-way ANOVA test with Dunnett test as follow-up test. The correlations were performed using Pearson and Spearman correlations as appropriate. A p value of 0.05 or less was considered significant.

RESULTS

LC–MS/MS method development

The second-tier LC-MS/MS method developed in NPC newborn screening was used for plasma TCG diagnostic assay, in which all the interferences in plasma to TCG can be baseline separated (30). Similar to NPC newborn screening assay, the protein precipitation with acetonitrile under basic condition was used to extract TCG from plasma. TCG was stable under basic condition.

Although umbilical cord blood plasma from many normal donors contain undetectable TCG and can serve as an ideal matrix for standard curve, we used inexpensive 2% CHAPS solution as surrogate matrix for standard curve. A surrogate matrix should be free of TCG and interferences, and the TCG should be stable in surrogate matrix. More importantly, responsiveness of TCG in surrogate matrix should be same as in plasma, which was demonstrated by parallelism of standard curves prepared in surrogate matrix and plasma (*vide infra*). The 2% CHAPS met above requirements and was chosen as surrogate matrix.

LC–MS/MS method validation

The bioanalytical method validation was conducted according to general procedures and criteria (40), and the following parameters were evaluated: recovery, matrix effect, parallelism of standard curves prepared in surrogate and authentic matrices, selectivity, sensitivity, accuracy, precision, linearity of the calibration curve, reproducibility of intra- and inter-assay, dilution integrity, stability at various conditions, and effect of hemolysis.

Extraction efficiency and matrix effects—To evaluate the recoveries of TCG from human plasma and surrogate standard curve matrix (2% CHAPS), signals of [$^{13}C_2$, ^{15}N]-TCG from pre-extraction spiked samples were compared to those of post-extraction spiked samples. The [$^{13}C_2$, ^{15}N]-TCG is a stable isotope-labeled analog of TCG. Both [$^{13}C_2$, ^{15}N]-TCG and TCG have same physicochemical properties including extraction recovery. The recoveries of TCG from human plasma and 2% CHAPS were 109% and 101%, respectively. The matrix factors (41) for TCG were assessed by comparing the peak response of the [$^{13}C_2$, ^{15}N]-TCG from post-extraction spiked samples to equivalent pure compound solutions in

acetonitrile-water (1:1). Matrix factors were 1.02 in both human plasma and 2% CHAPS, suggesting that there are no significant matrix effects for TCG in these matrices.

Parallelism of standard curves in surrogate and authentic matrices—To apply standard curve in surrogate matrix, it is essential to establish parallelism between surrogate and authentic matrix standard curves. The standard curve prepared in human plasma were parallel to that prepared in 2% CHAPS solution, and the differences in slopes of the standard curves in surrogate and authentic matrices was less than 5%. The result suggested that the same responsiveness of TCG in different matrices was observed, and calibration curve prepared in 2% CHAPS was suitable for analysis of plasma samples.

Selectivity

To ascertain the method selectivity, blank (2% CHAPS solution) with and without internal standard and human plasma samples from six subjects including control and NPC subjects were analyzed. As shown in Figure 2A, no interfering peaks to analyte and internal standard from blanks were observed. There are no interfering peaks to analyte from blank with internal standard (Figure 2B). In the highest calibrator (ULOQ, 1000 ng/mL) without internal standards, there are no interfering peaks to internal standard (data not shown). Plasma without internal standard used in the validation showed no interference peaks at the retention time of internal standard (Figure 2C). Control plasma contained low level of TCG (Figure 2D), whereas in NPC1 plasma very high level of TCG was present (Figure 2E).

Sensitivity

The LLOQ for TCG was prepared in 2% CHAPS solution at 1 ng/mL. The LLOQ samples were processed and analyzed with a calibration curve and QC samples (Table 1). The intra-run accuracy and precision were −5.0 – −2.8% RE and 5.7 – 7.7% CV, respectively. The inter-run accuracy and precision were −3.7% RE and 6.4% CV, respectively. A typical MRM chromatogram at the LLOQ concentration is shown in Figure 2F.

Accuracy and precision

The accuracy and precision of the method were assessed by analyzing QC samples along with a calibration curve on three different days. In each run, for the calibration standards ranging from 1 to 1000 ng/mL, the deviations of the back-calculated concentrations from their nominal values were within ±15.0%. The intra-assay %CV, based on five levels of analytical QCs (LLQC, LQC, MQC, HQC, and DQC), was within 5.7%; the inter-assay precision (%CV) was within 5.0%, and the intra- and inter-assay accuracy were within ±5.2%RE and ±3.6%RE, respectively (Table 1).

Stability

Stability of the TCG in the human plasma was evaluated under a variety of conditions to establish length of storage and sample processing conditions. The bench-top stability study showed that the TCG was stable in human plasma for 5 days at room temperature and 37 °C. The stability of TCG was determined to be acceptable in human plasma following five freeze-thaw cycles. For processed samples (autosampler stability), the TCG were stable for 3

days at 4 °C. The TCG was determined to be stable for 448 days at −80 °C in human plasma. The TCG in whole blood was stable at 4 °C and room temperature for 18 hours.

The TCG in standard curve matrix was stable for 24 hours at room temperature and for 448 days at −80 °C. In stock solution, TCG was stable for 24 hours at room temperature and for 90 days at −20 °C.

Carryover and run size evaluation

To evaluate carryover, a blank sample was immediately injected following the highest standard (1000 ng/mL TCG). No carryover was observed in the regions of interest. The assay was validated to successfully analyze batch size of 226 samples and all the QC samples met accuracy and precision requirements.

Effect of hemolysis

The hemolyzed plasma with hemoglobin up to 800 mg/dL did not have negative effect on accuracy.

Establishment of cut-off value for diagnosis

We used the validated plasma TCG assay to establish the cut-off value for NPC1 diagnosis. Plasma samples from 183 previously diagnosed NPC1 subjects, 52 obligate NPC1 carriers, and 130 non-NPC1 control subjects were analyzed. The reference ranges for NPC1, NPC1 carrier, and control subjects were 10.1 - 897 ng/mL, < 1 - 43.3 ng/, and < 1 - 6.8 ng/mL, respectively (Figure 3A). Receiver-operator curve (ROC) analysis demonstrated that the area under the curve for TCG is 0.9999. The assay with cutoff value of 18.5 ng/mL has sensitivity of 0.9945 and specificity of 0.9982 (Figure 3B). Only one neurologically asymptomatic adult who is a presumptive NPC1 subject that carries a high frequency variant (c.665A>C, p.N222S) (42) showed TCG level below the cutoff.

To assess specificity of the assay, we examined patient samples from other genetic disorders, including Fabry, FH, Gaucher, Krabbe, CTX, GM1, GM2, SPG5, MPS I, II, IIIA, IIIB, IIIC, IVA, VI, VII, Batten, ML II/III, lysosomal acid lipase deficiency (LALD) including CESD and Wolman, ASMD, and ASMD carriers. TCG in ASMD, CESD and Wolman disease was above the cutoff (18.5 ng/mL) for NPC1 disease (Figure 3C and D). In the NPC1 natural history study, longitudinal samples were collected from 11 participants over 9 - 48 months of study period. The TCG levels in 91% of participants during study were quite steady (%CV < 33%) (Figure 3E). The mean plasma TCG level for female NPC1 subjects was 31% lower than male subjects ($P < 0.01$) (Figure 3F), similar to dried blood spot TCG level (30). The plasma TCG levels were not significantly correlated with NPC neurological disease severity scores (43) (r = 0.1474, p = 0.9216) (Figure 3G) or NPC neurological annual severity increment scores (44) (r =0.0701, p = 0.8414) (Figure 3H).

Comparison of TCG with C-triol and PPCS in diagnosis of NPC1 disease

We have developed diagnostic tests for NPC1 disease based on plasma C-triol (7), PPCS (29), and TCG, and used these tests in clinical diagnosis. There were significant correlations between the bile acid and C-triol (r = 0.64, p < 0.0001) (Figure 4A) and between the bile

acid and PPCS ($r = 0.55$, $p < 0.0001$) (Figure 4B). Here we compare their performances in diagnosis of 301 consecutive, unknown patients for samples submitted to the Washington University Metabolomics Core from 2016 to 2020. All the NPC1 patients were successfully identified by these biomarkers. C-triol (Figure 4C), PPCS (Figure 4D), TCG (Figure 4D) misdiagnosed 11, 4, and 1 non-NPC1 subjects, respectively, in which diagnosis of NPC was excluded by genetic testing in 8 subjects. These results indicated that these three biomarkers were equally sensitive in detection of NPC1 patients, but that TCG was more specific.

Application of TCG to assessment of treatment with miglustat in NPC1 disease

Miglustat, an inhibitor of glycosylceramide syhthesis, is used off-label to treat patients with NPC. Pre- and post-miglustat treatment plasma samples were collected from 9 NPC1 participants who were followed in the NPC history study, thus providing an opportunity to examine the effect of miglustat on the plasma TCG levels. The participants were treated with 200 mg miglustat three times a day adjusted for body surface area in children [(body surface area/1.8) × 600] (45). No significant differences were found in plasma TCG between pre- and post-treatment (Figure 5A), and the plasma TCG levels are 9-fold above the NPC1 cutoff (Figure 5B).

Application of TCG to assessment of treatment with HPβCD in NPC1 disease

Systemic and intrathecal (IT) administrations of HPβCD to NPC1 mouse (46-48) and cat (49) models, respectively, ameliorated neurological symptoms and prolonged life, leading to expanded access use in NPC1 patients. IT HPβCD treatment in NPC1 subjects slowed the neurological disease progression (34, 35, 37), and IV treatment improved the liver disease (38, 39). We evaluated the responses of plasma TCG to IT and IV HPβCD treatment in NPC1 patients. The plasma TCG levels in 18 NPC1 participants showed large variations during the Phase 1/2a trial of IT HPβCD (Figure 6A - C), and an average of 15% decrease of TCG was observed at the end of trial ($P < 0.05$) (Figure 6D), though TCG levels in all the participants were still at least 2.3-fold above the NPC1 cutoff at the last visit (Figure 6E). IV HPβCD treatment led to more than 60% reduction of plasma TCG in patients 1 and 2 whose levels were within normal range, and 56% reduction in patient 3 (Figure 6F). These results suggest that plasma TCG primarily reflects peripheral disease and is a suitable pharmacodynamic/response biomarker for IV HPβCD treatment.

DISCUSSION

Diagnosis of NPC is challenging because of the non-specific early symptoms and wide range of age of onset of clinical disease (3). Both biomarker profiling and gene testing are included as first-line diagnostic tests to identify NPC (4, 22, 50). A variety of biomarkers with diagnostic potential have been reported (4, 51), including plasma C-triol (5, 7, 9-15, 17-20), 7-ketocholesterol (7, 8, 16), PPCS (20, 21, 23-29), lysosphingomyelin (25, 26, 52), dried blood spot TCG (30, 31), urine di-22:6-bis(monoacylglycerol)phosphate (53), and urine 3β-sulfooxy-7β-hydroxy-5-cholenoic acid (28, 54, 55). Among these, plasma C-triol (7, 13, 14), 7-ketocholesterol (7, 14), PPCS (23, 29), and dried blood spot TCG (30) were studied extensively and showed high sensitivity and varying specificity to differentiate NPC1 from NPC1 carriers and controls. In this study, we developed a plasma TCG diagnostic

assay that also showed high sensitivity to discriminate NPC1 from NPC1 carriers and controls. C-triol and 7-ketocholesterol are the first NPC diagnostic biomarkers that have been most widely used. C-triol is superior to 7-ketocholesterol due to higher specificity (9, 11, 22) and has been recommended as first line NPC diagnostic biomarker (4, 22, 50). C-triol was found to be elevated in other genetic disorders including ASMD, CTX, and LALD (10, 11, 14, 22); TCG is elevated in ASMD and LALD; and PPCS is only increased in ASMD (25, 26, 29). Study of TCG, C-triol, and PPCS for diagnosis of NPC1 from unknown patients showed that they were equally sensitive, and TCG was the most specific. This is in agreement with their specificity of 0.9982, 0.8857 (14, 23), and 0.9663 (29) to distinguish NPC1 from NPC1 carriers and controls, respectively. Compared to C-triol and PPCS, TCG showed remarkable stability in plasma. C-triol was elevated due to autooxidation of cholesterol when the plasma sample was stored at room temperature for more than 24 hours (7, 13), and PPCS was artifictually produced when plasma was dried on newborn screening card (29). TCG was stable in plasma at room temperature and even 37 °C for 5 days, suggesting that the shipment of plasma sample for TCG assay with dry ice during mild weather is not necessary. Derivatization of C-triol was required to achieve enough sensitivity, and we found that C-triol was artifictually generated during the derivatization when cholesterol and 5,6-epoxycholesterol were not completely removed. The TCG assay is easier to set up than C-triol assay in a clinical lab, as TCG can be easily detected without derivatization. These technical advantages of TCG allowed us to measure TCG more accurate than C-triol, which is important to diagnose patients with marker marginally close to cutoff. Based on these results, we expect that TCG will replace C-triol as first line NPC diagnostic biomarker in the future. C-triol is generated from oxidation of cholesterol due to oxidative stress in NPC disease (8), which is further metabolized to TCG (30). C-triol was able to identify NPC2 patients (15) (18), suggesting TCG may also be able to diagnose NPC2, though this was not explored in the current study. PPCS represents a novel class of lipids that are generated through an unknown metabolic pathway. Application of TCG and PPCS should provide complementary results to enhance the NPC diagnosis.

The deficiency of NPC1 protein results in accumulation of unesterified cholesterol in lysosomes leading to progressive neurodegeneration and liver disease in early life. Although the cholestatic liver disease in many NPC infants resolves without intervention, the sub-clinical liver disease such as hepatomegaly often remains for a variable period of time (3), and the liver disease of NPC can develop into hepatocellular carcinoma (56-58). Cholesterol is markedly elevated in livers of NPC animal models (49, 59, 60) and patients (61). The oxidative stress (62-64) in NPC disease leads to oxidization of trapped cholesterol to 5,6-epoxycholesterol that is further hydrolyzed under acidic condition in lysosomes (65) to C-triol (17), which is further metabolized to TCG in liver (30). These biomarkers are principally generated in the liver and can serve as biomarkers to monitor oxidizable pools of cholesterol in that tissue. Systemic administration of HPβPD to NPC1 mice (46-48, 66) and cat (49) models has been shown to mobilize trapped cholesterol from lysosomes and normalize cholesterol levels in the liver. The administration of IV HPβCD showed benefits such as improved hepatomegaly and transaminase levels in NPC1 patients (38, 39). In line with treatment benefits, we observed significant reduction of plasma C-triol (67) and TCG levels in NPC1 participants after IV HPβCD treatment. A limitation of current study is that

no liver disease data were collected. An IV HPβCD clinical trial showed that reduction of TCG was correlated with reductions of alanine transaminase and aspartate aminotransferase levels, direct bilirubin, and total bilirubin, and the results were submitted for publication in a separated paper. By contrast, the low doses (50 – 200 mg) of HPβCD used in IT treatment (35, 37), compared to IV doses (500 - 2000 mg/kg), did not reach sufficient blood concentrations to effectively reduce cholesterol levels in the liver in most of the participants, leading to modest responses of TCG to treatment. Miglustat, an inhibitor of glycosphingolipid biosysnthesis, neither reduces lysosomal accumulation of cholesterol (68) nor ameliorates oxidative stress (64), and treatment with this drug had no significant effect on the plasma TCG.

In summary, we developed a LC–MS/MS diagnostic assay based on plasma TCG with sensitivity of 0.9945 and specificity of 0.9982 to differentiate NPC1 from NPC1 carriers and controls. Compared to other commonly used NPC1 biomarkers, C-triol and PPCS, TCG was equally sensitive but more specific. We expect that TCG will replace C-triol as the first line diagnostic biomarker for NPC disease. TCG may also be used to identify LALD and ASMD. We further found that TCG also can be used to monitor reduction of cholesterol storage in liver lysosomes following administration of IV HPβCD.

ACKNOWLEDGMENTS

This work was supported by grants from the National Niemann-Pick Disease Foundation (X.J.), the NIH CTSA Grant # UL1 TR000448 (X.J.), Together Strong NPC Foundation (X.J.), the University of Pennsylvania Orphan Disease Center (MDBR-17-124-NPC, X.J.), Dana's Angels Research Trust (D.S.O. and N.M.Y.), Ara Parseghian Medical Research Foundation (D.S.O., N.M.Y., and X.J.), Support of Accelerated Research for NPC Disease (D.S.O.), Hope for Hayley and Samantha's Search for the Cure Funds (E.B.K.), the Liferay Foundation and the Campbell Foundation of Caring (R.Y.W.), and by NIH grants R01 NS081985 (D.S.O. and J.E.S.) and U01 HD090845 (D.S.O. and X.J.). This study was also supported by the intramural research program of the *Eunice Kennedy Shriver* National Institute of Child Health and Human Development (F.D.P.), a Bench to Bedside award from the Office of Rare Diseases (F.D.P. and D.S.O.), and National Center for Advancing Translational Sciences grant 1ZIATR000014 (F.D.P.). This work was performed in the Metabolomics Facility at Washington University (NIH P30 DK020579). We are grateful to the National Niemann-Pick Disease Foundation for their assistance in obtaining samples from NPC1 and NPC1 carrier subjects. The authors express their appreciation to the families and patients who participated in this study. The content is solely the responsibility of the authors and does not necessarily represent the official views of the National Institutes of Health.

Abbreviations:

ASMD	acid-sphingomyelinase deficiency
CESD	cholesteryl ester storage disease
CHAPS	3-[(3-cholamidopropyl)dimethylammonio]-1-propanesulfonate
C-triol	cholestane-3β,5α,6β-triol
CTX	cerebrotendineous xanthomathosis
%CV	percent coefficient of variance
DQC	dilution quality control
FH	familial hypercholesterolemia

GM1	GM1 gangliosidosis
GM2	GM2 gangliosidosis
H-HQC	hemolyzed high quality control
HILIC	hydrophilic interaction chromatography
H-LQC	hemolyzed low quality control
HPβCD	2-hydroxypropyl-β-cyclodextrin
HPLC	high performance liquid chromatography
HQC	high quality control
IT	intrathecal
IV	intravenous
LALD	lysosomal acid lipase deficiency
LC-MS/MS	liquid chromatography-tandem mass spectrometry
LLOQ	lower limit of quantification
LLQC	lower limit quality control
LQC	low quality control
ML	mucolipidosis
MPS	mucopolysaccharidosis
MQC	middle quality control
MRM	multiple reaction monitoring
NPC	Niemann-Pick type C
PPCS	N-palmitoyl-O-phosphocholineserine
QC	quality control
%RE	percent relative error
ROC	receiver-operator characteristic
RUMC	Rush University Medical Center
SD	standard deviation
SDS	sodium dodecyl sulfate
SPG5	spastic paraplegia type 5
TCG	(3β,5α,6β-trihydroxy-cholan-24-oyl)glycine

ULOQ upper limit of quantification

REFERENCES

1. Carstea ED, Morris JA, Coleman KG, Loftus SK, Zhang D, Cummings C, Gu J, Rosenfeld MA, Pavan WJ, Krizman DB, Nagle J, Polymeropoulos MH, Sturley SL, Ioannou YA, Higgins ME, Comly M, Cooney A, Brown A, Kaneski CR, Blanchette-Mackie EJ, Dwyer NK, Neufeld EB, Chang TY, Liscum L, Strauss JF 3rd, Ohno K, Zeigler M, Carmi R, Sokol J, Markie D, O'Neill RR, van Diggelen OP, Elleder M, Patterson MC, Brady RO, Vanier MT, Pentchev PG, and Tagle DA. 1997. Niemann-Pick C1 disease gene: homology to mediators of cholesterol homeostasis. Science 277: 228–231. [PubMed: 9211849]
2. Naureckiene S, Sleat DE, Lackland H, Fensom A, Vanier MT, Wattiaux R, Jadot M, and Lobel P. 2000. Identification of HE1 as the second gene of Niemann-Pick C disease. Science 290: 2298–2301. [PubMed: 11125141]
3. Vanier MT 2010. Niemann-Pick disease type C. Orphanet J Rare Dis 5: 16. [PubMed: 20525256]
4. Vanier MT, Gissen P, Bauer P, Coll MJ, Burlina A, Hendriksz CJ, Latour P, Goizet C, Welford RW, Marquardt T, and Kolb SA. 2016. Diagnostic tests for Niemann-Pick disease type C (NP-C): A critical review. Mol Genet Metab 118: 244–254. [PubMed: 27339554]
5. Bauer P, Balding DJ, Klunemann HH, Linden DE, Ory DS, Pineda M, Priller J, Sedel F, Muller A, Chadha-Boreham H, Welford RW, Strasser DS, and Patterson MC. 2013. Genetic screening for Niemann-Pick disease type C in adults with neurological and psychiatric symptoms: findings from the ZOOM study. Hum Mol Genet 22: 4349–4356. [PubMed: 23773996]
6. Patterson MC, Clayton P, Gissen P, Anheim M, Bauer P, Bonnot O, Dardis A, Dionisi-Vici C, Klunemann HH, Latour P, Lourenco CM, Ory DS, Parker A, Pocovi M, Strupp M, Vanier MT, Walterfang M, and Marquardt T. 2017. Recommendations for the detection and diagnosis of Niemann-Pick disease type C: An update. Neurol Clin Pract 7: 499–511. [PubMed: 29431164]
7. Jiang X, Sidhu R, Porter FD, Yanjanin NM, Speak AO, te Vruchte DT, Platt FM, Fujiwara H, Scherrer DE, Zhang J, Dietzen DJ, Schaffer JE, and Ory DS. 2011. A sensitive and specific LC-MS/MS method for rapid diagnosis of Niemann-Pick C1 disease from human plasma. J Lipid Res 52: 1435–1445. [PubMed: 21518695]
8. Porter FD, Scherrer DE, Lanier MH, Langmade SJ, Molugu V, Gale SE, Olzeski D, Sidhu R, Dietzen DJ, Fu R, Wassif CA, Yanjanin NM, Marso SP, House J, Vite C, Schaffer JE, and Ory DS. 2010. Cholesterol oxidation products are sensitive and specific blood-based biomarkers for Niemann-Pick C1 disease. Sci Transl Med 2: 56ra81.
9. Boenzi S, Deodato F, Taurisano R, Martinelli D, Verrigni D, Carrozzo R, Bertini E, Pastore A, Dionisi-Vici C, and Johnson DW. 2014. A new simple and rapid LC-ESI-MS/MS method for quantification of plasma oxysterols as dimethylaminobutyrate esters. Its successful use for the diagnosis of Niemann-Pick type C disease. Clin Chim Acta 437: 93–100. [PubMed: 25038260]
10. Klinke G, Rohrbach M, Giugliani R, Burda P, Baumgartner MR, Tran C, Gautschi M, Mathis D, and Hersberger M. 2015. LC-MS/MS based assay and reference intervals in children and adolescents for oxysterols elevated in Niemann-Pick diseases. Clin Biochem 48: 596–602. [PubMed: 25819840]
11. Pajares S, Arias A, Garcia-Villoria J, Macias-Vidal J, Ros E, de las Heras J, Giros M, Coll MJ, and Ribes A. 2015. Cholestane-3beta,5alpha,6beta-triol: high levels in Niemann-Pick type C, cerebrotendinous xanthomatosis, and lysosomal acid lipase deficiency. J Lipid Res 56: 1926–1935. [PubMed: 26239048]
12. Kannenberg F, Nofer JR, Schulte E, Reunert J, Marquardt T, and Fobker M. 2017. Determination of serum cholestane-3beta,5alpha,6beta-triol by gas chromatography-mass spectrometry for identification of Niemann-Pick type C (NPC) disease. J Steroid Biochem Mol Biol 169: 54–60. [PubMed: 26940355]
13. Reunert J, Fobker M, Kannenberg F, Du Chesne I, Plate M, Wellhausen J, Rust S, and Marquardt T. 2016. Rapid Diagnosis of 83 Patients with Niemann Pick Type C Disease and Related Cholesterol Transport Disorders by Cholestantriol Screening. EBioMedicine 4: 170–175. [PubMed: 26981555]

14. Romanello M, Zampieri S, Bortolotti N, Deroma L, Sechi A, Fiumara A, Parini R, Borroni B, Brancati F, Bruni A, Russo CV, Bordugo A, Bembi B, and Dardis A. 2016. Comprehensive Evaluation of Plasma 7-Ketocholesterol and Cholestan-3beta,5alpha,6beta-Triol in an Italian Cohort of Patients Affected by Niemann-Pick Disease due to NPC1 and SMPD1 Mutations. Clin Chim Acta 455: 39–45. [PubMed: 26790753]
15. Reunert J, Lotz-Havla AS, Polo G, Kannenberg F, Fobker M, Griese M, Mengel E, Muntau AC, Schnabel P, Sommerburg O, Borggraefe I, Dardis A, Burlina AP, Mall MA, Ciana G, Bembi B, Burlina AB, and Marquardt T. 2015. Niemann-Pick Type C-2 Disease: Identification by Analysis of Plasma Cholestane-3beta,5alpha,6beta-Triol and Further Insight into the Clinical Phenotype. JIMD Rep 23: 17–26. [PubMed: 25772320]
16. Zhang H, Wang Y, Lin N, Yang R, Qiu W, Han L, Ye J, and Gu X. 2014. Diagnosis of Niemann-Pick disease type C with 7-ketocholesterol screening followed by NPC1/NPC2 gene mutation confirmation in Chinese patients. Orphanet J Rare Dis 9: 82. [PubMed: 24915861]
17. Hammerschmidt TG, de Oliveira Schmitt Ribas G, Saraiva-Pereira ML, Bonatto MP, Kessler RG, Souza FTS, Trapp F, Michelin-Tirelli K, Burin MG, Giugliani R, and Vargas CR. 2017. Molecular and biochemical biomarkers for diagnosis and therapy monitorization of Niemann-Pick type C patients. Int J Dev Neurosci 66: 18–23. [PubMed: 29197565]
18. Polo G, Burlina A, Furlan F, Kolamunnage T, Cananzi M, Giordano L, Zaninotto M, Plebani M, and Burlina A. 2016. High level of oxysterols in neonatal cholestasis: a pitfall in analysis of biochemical markers for Niemann-Pick type C disease. Clin Chem Lab Med 54: 1221–1229. [PubMed: 26650075]
19. Ribas GS, Souza HM, de Mari J, Deon M, Mescka C, Saraiva-Pereira ML, Kessler R, Trapp F, Michelin K, Burin M, Vargas CR, and Giugliani R. 2016. Selective screening of Niemann-Pick type C Brazilian patients by cholestane-3beta,5alpha,6beta-triol and chitotriosidase measurements followed by filipin staining and NPC1/NPC2 gene analysis. Clin Chim Acta 459: 57–62. [PubMed: 27234403]
20. Deodato F, Boenzi S, Taurisano R, Semeraro M, Sacchetti E, Carrozzo R, and Dionisi-Vici C. 2018. The impact of biomarkers analysis in the diagnosis of Niemann-Pick C disease and acid sphingomyelinase deficiency. Clin Chim Acta 486: 387–394. [PubMed: 30153451]
21. Voorink-Moret M, Goorden SMI, van Kuilenburg ABP, Wijburg FA, Ghauharali-van der Vlugt JMM, Beers-Stet FS, Zoetekouw A, Kulik W, Hollak CEM, and Vaz FM. 2018. Rapid screening for lipid storage disorders using biochemical markers. Expert center data and review of the literature. Mol Genet Metab 123: 76–84. [PubMed: 29290526]
22. Boenzi S, Deodato F, Taurisano R, Goffredo BM, Rizzo C, and Dionisi-Vici C. 2016. Evaluation of plasma cholestane-3beta,5alpha,6beta-triol and 7-ketocholesterol in inherited disorders related to cholesterol metabolism. J Lipid Res 57: 361–367. [PubMed: 26733147]
23. Giese AK, Mascher H, Grittner U, Eichler S, Kramp G, Lukas J, te Vruchte D, Al Eisa N, Cortina-Borja M, Porter FD, Platt FM, and Rolfs A. 2015. A novel, highly sensitive and specific biomarker for Niemann-Pick type C1 disease. Orphanet J Rare Dis 10: 78. [PubMed: 26082315]
24. Kuchar L, Sikora J, Gulinello ME, Poupetova H, Lugowska A, Malinova V, Jahnova H, Asfaw B, and Ledvinova J. 2017. Quantitation of plasmatic lysosphingomyelin and lysosphingomyelin-509 for differential screening of Niemann-Pick A/B and C diseases. Anal Biochem 525: 73–77. [PubMed: 28259515]
25. Pettazzoni M, Froissart R, Pagan C, Vanier MT, Ruet S, Latour P, Guffon N, Fouilhoux A, Germain DP, Levade T, Vianey-Saban C, Piraud M, and Cheillan D. 2017. LC-MS/MS multiplex analysis of lysosphingolipids in plasma and amniotic fluid: A novel tool for the screening of sphingolipidoses and Niemann-Pick type C disease. PLoS One 12: e0181700. [PubMed: 28749998]
26. Polo G, Burlina AP, Kolamunnage TB, Zampieri M, Dionisi-Vici C, Strisciuglio P, Zaninotto M, Plebani M, and Burlina AB. 2017. Diagnosis of sphingolipidoses: a new simultaneous measurement of lysosphingolipids by LC-MS/MS. Clin Chem Lab Med 55: 403–414. [PubMed: 27533120]
27. Polo G, Burlina AP, Ranieri E, Colucci F, Rubert L, Pascarella A, Duro G, Tummolo A, Padoan A, Plebani M, and Burlina AB. 2019. Plasma and dried blood spot lysosphingolipids for the diagnosis of different sphingolipidoses: a comparative study. Clin Chem Lab Med.

28. Mashima R, Maekawa M, Narita A, Okuyama T, and Mano N. 2018. Elevation of plasma lysosphingomyelin-509 and urinary bile acid metabolite in Niemann-Pick disease type C-affected individuals. Mol Genet Metab Rep 15: 90–95. [PubMed: 30023294]

29. Sidhu R, Kell P, Dietzen DJ, Farhat NY, Do AND, Porter FD, Berry-Kravis E, Vite CH, Reunert J, Marquardt T, Giugliani R, Lourenco CM, Bodamer O, Wang RY, Plummer E, Schaffer JE, Ory DS, and Jiang X. 2020. Application of N-palmitoyl-O-phosphocholineserine for diagnosis and assessment of response to treatment in Niemann-Pick type C disease. Mol Genet Metab.

30. Jiang X, Sidhu R, Mydock-McGrane L, Hsu FF, Covey DF, Scherrer DE, Earley B, Gale SE, Farhat NY, Porter FD, Dietzen DJ, Orsini JJ, Berry-Kravis E, Zhang X, Reunert J, Marquardt T, Runz H, Giugliani R, Schaffer JE, and Ory DS. 2016. Development of a bile acid-based newborn screen for Niemann-Pick disease type C. Sci Transl Med 8: 337ra363.

31. Mazzacuva F, Mills P, Mills K, Camuzeaux S, Gissen P, Nicoli ER, Wassif C, Te Vruchte D, Porter FD, Maekawa M, Mano N, Iida T, Platt F, and Clayton PT. 2016. Identification of novel bile acids as biomarkers for the early diagnosis of Niemann-Pick C disease. FEBS Lett 590: 1651–1662. [PubMed: 27139891]

32. Sidhu R, Mondjinou Y, Qian M, Song H, Kumar AB, Hong X, Hsu FF, Dietzen DJ, Yanjanin NM, Porter FD, Berry-Kravis E, Vite CH, Gelb MH, Schaffer JE, Ory DS, and Jiang X. 2019. N-Acyl-O-phosphocholineserines: structures of a novel class of lipids that are biomarkers for Niemann-Pick C1 disease. J Lipid Res.

33. Jiang X, Sidhu R, Orsini JJ, Farhat NY, Porter FD, Berry-Kravis E, Schaffer JE, and Ory DS. 2019. Diagnosis of niemann-pick C1 by measurement of bile acid biomarkers in archived newborn dried blood spots. Mol Genet Metab 126: 183–187. [PubMed: 30172462]

34. Maarup TJ, Chen AH, Porter FD, Farhat NY, Ory DS, Sidhu R, Jiang X, and Dickson PI. 2015. Intrathecal 2-hydroxypropyl-beta-cyclodextrin in a single patient with Niemann-Pick C1. Mol Genet Metab 116: 75–79. [PubMed: 26189084]

35. Berry-Kravis E, Chin J, Hoffmann A, Winston A, Stoner R, LaGorio L, Friedmann K, Hernandez M, Ory DS, Porter FD, and O'Keefe JA. 2018. Long-Term Treatment of Niemann-Pick Type C1 Disease With Intrathecal 2-Hydroxypropyl-Beta-Cyclodextrin. Pediatr Neurol.

36. Garcia-Robles AA, Company-Albir MJ, Megias-Vericat JE, Fernandez-Megia MJ, Perez-Miralles FC, Lopez-Briz E, Alcala-Vicente C, Galeano I, Casanova B, and Poveda JL. 2016. Use of 2 hydroxypropyl-beta-cyclodextrin therapy in two adult Niemann Pick Type C patients. J Neurol Sci 366: 65–67. [PubMed: 27288778]

37. Ory DS, Ottinger EA, Farhat NY, King KA, Jiang X, Weissfeld L, Berry-Kravis E, Davidson CD, Bianconi S, Keener LA, Rao R, Soldatos A, Sidhu R, Walters KA, Xu X, Thurm A, Solomon B, Pavan WJ, Machielse BN, Kao M, Silber SA, McKew JC, Brewer CC, Vite CH, Walkley SU, Austin CP, and Porter FD. 2017. Intrathecal 2-hydroxypropyl-beta-cyclodextrin decreases neurological disease progression in Niemann-Pick disease, type C1: a non-randomised, open-label, phase 1-2 trial. Lancet 390: 1758–1768. [PubMed: 28803710]

38. Matsuo M, Togawa M, Hirabaru K, Mochinaga S, Narita A, Adachi M, Egashira M, Irie T, and Ohno K. 2013. Effects of cyclodextrin in two patients with Niemann-Pick Type C disease. Mol Genet Metab 108: 76–81. [PubMed: 23218948]

39. Hastings C, Vieira C, Liu B, Bascon C, Gao C, Wang RY, Casey A, and Hrynkow S. 2019. Expanded access with intravenous hydroxypropyl-beta-cyclodextrin to treat children and young adults with Niemann-Pick disease type C1: a case report analysis. Orphanet J Rare Dis 14: 228. [PubMed: 31639011]

40. US Department of Health and Human Services, F., Center for Drug Evaluation and Research and Center for Veterinary Medicine. Guidance for Industry: Bioanalytical Method Validations. 5 2018. 2018.

41. Viswanathan CT, Bansal S, Booth B, DeStefano AJ, Rose MJ, Sailstad J, Shah VP, Skelly JP, Swann PG, and Weiner R. 2007. Quantitative bioanalytical methods validation and implementation: best practices for chromatographic and ligand binding assays. Pharm Res 24: 1962–1973. [PubMed: 17458684]

42. Wassif CA, Cross JL, Iben J, Sanchez-Pulido L, Cougnoux A, Platt FM, Ory DS, Ponting CP, Bailey-Wilson JE, Biesecker LG, and Porter FD. 2016. High incidence of unrecognized visceral/

neurological late-onset Niemann-Pick disease, type C1, predicted by analysis of massively parallel sequencing data sets. Genet Med 18: 41–48. [PubMed: 25764212]

43. Yanjanin NM, Velez JI, Gropman A, King K, Bianconi SE, Conley SK, Brewer CC, Solomon B, Pavan WJ, Arcos-Burgos M, Patterson MC, and Porter FD. 2010. Linear clinical progression, independent of age of onset, in Niemann-Pick disease, type C. Am J Med Genet B Neuropsychiatr Genet 153B: 132–140. [PubMed: 19415691]
44. te Vruchte D, Speak AO, Wallom KL, Al Eisa N, Smith DA, Hendriksz CJ, Simmons L, Lachmann RH, Cousins A, Hartung R, Mengel E, Runz H, Beck M, Amraoui Y, Imrie J, Jacklin E, Riddick K, Yanjanin NM, Wassif CA, Rolfs A, Rimmele F, Wright N, Taylor C, Ramaswami U, Cox TM, Hastings C, Jiang X, Sidhu R, Ory DS, Arias B, Jeyakumar M, Sillence DJ, Wraith JE, Porter FD, Cortina-Borja M, and Platt FM. 2014. Relative acidic compartment volume as a lysosomal storage disorder-associated biomarker. J Clin Invest 124: 1320–1328. [PubMed: 24487591]
45. Bradbury A, Bagel J, Sampson M, Farhat N, Ding W, Swain G, Prociuk M, O'Donnell P, Drobatz K, Gurda B, Wassif C, Remaley A, Porter F, and Vite C. 2016. Cerebrospinal Fluid Calbindin D Concentration as a Biomarker of Cerebellar Disease Progression in Niemann-Pick Type C1 Disease. J Pharmacol Exp Ther 358: 254–261. [PubMed: 27307499]
46. Ramirez CM, Liu B, Taylor AM, Repa JJ, Burns DK, Weinberg AG, Turley SD, and Dietschy JM. 2010. Weekly cyclodextrin administration normalizes cholesterol metabolism in nearly every organ of the Niemann-Pick type C1 mouse and markedly prolongs life. Pediatr Res 68: 309–315. [PubMed: 20581737]
47. Lopez AM, Terpack SJ, Posey KS, Liu B, Ramirez CM, and Turley SD. 2014. Systemic administration of 2-hydroxypropyl-beta-cyclodextrin to symptomatic Npc1-deficient mice slows cholesterol sequestration in the major organs and improves liver function. Clin Exp Pharmacol Physiol 41: 780–787. [PubMed: 25115571]
48. Tanaka Y, Yamada Y, Ishitsuka Y, Matsuo M, Shiraishi K, Wada K, Uchio Y, Kondo Y, Takeo T, Nakagata N, Higashi T, Motoyama K, Arima H, Mochinaga S, Higaki K, Ohno K, and Irie T. 2015. Efficacy of 2-Hydroxypropyl-beta-cyclodextrin in Niemann-Pick Disease Type C Model Mice and Its Pharmacokinetic Analysis in a Patient with the Disease. Biol Pharm Bull 38: 844–851. [PubMed: 26027824]
49. Vite CH, Bagel JH, Swain GP, Prociuk M, Sikora TU, Stein VM, O'Donnell P, Ruane T, Ward S, Crooks A, Li S, Mauldin E, Stellar S, De Meulder M, Kao ML, Ory DS, Davidson C, Vanier MT, and Walkley SU. 2015. Intracisternal cyclodextrin prevents cerebellar dysfunction and Purkinje cell death in feline Niemann-Pick type C1 disease. Sci Transl Med 7: 276ra226.
50. Geberhiwot T, Moro A, Dardis A, Ramaswami U, Sirrs S, Marfa MP, Vanier MT, Walterfang M, Bolton S, Dawson C, Heron B, Stampfer M, Imrie J, Hendriksz C, Gissen P, Crushell E, Coll MJ, Nadjar Y, Klunemann H, Mengel E, Hrebicek M, Jones SA, Ory D, Bembi B, Patterson M, and International Niemann-Pick Disease R. 2018. Consensus clinical management guidelines for Niemann-Pick disease type C. Orphanet J Rare Dis 13: 50. [PubMed: 29625568]
51. Sitarska D, and Lugowska A. 2019. Laboratory diagnosis of the Niemann-Pick type C disease: an inherited neurodegenerative disorder of cholesterol metabolism. Metab Brain Dis 34: 1253–1260. [PubMed: 31197681]
52. Welford RW, Garzotti M, Marques Lourenco C, Mengel E, Marquardt T, Reunert J, Amraoui Y, Kolb SA, Morand O, and Groenen P. 2014. Plasma lysosphingomyelin demonstrates great potential as a diagnostic biomarker for Niemann-Pick disease type C in a retrospective study. PLoS One 9: e114669. [PubMed: 25479233]
53. Liu N, Tengstrand EA, Chourb L, and Hsieh FY. 2014. Di-22:6-bis(monoacylglycerol)phosphate: A clinical biomarker of drug-induced phospholipidosis for drug development and safety assessment. Toxicol Appl Pharmacol 279: 467–476. [PubMed: 24967688]
54. Maekawa M, Omura K, Sekiguchi S, Iida T, Saigusa D, Yamaguchi H, and Mano N. 2016. Identification of Two Sulfated Cholesterol Metabolites Found in the Urine of a Patient with Niemann-Pick Disease Type C as Novel Candidate Diagnostic Markers. Mass Spectrom (Tokyo) 5: S0053. [PubMed: 27900236]
55. Maekawa M, Jinnoh I, Narita A, Iida T, Saigusa D, Iwahori A, Nittono H, Okuyama T, Eto Y, Ohno K, Clayton PT, Yamaguchi H, and Mano N. 2019. Investigation of diagnostic performance

of five urinary cholesterol metabolites for Niemann-Pick disease type C. J Lipid Res 60: 2074–2081. [PubMed: 31586016]

56. Pennington DJ, Sivit CJ, and Chandra RS. 1996. Hepatocellular carcinoma in a child with Niemann-Pick disease: imaging findings. Pediatr Radiol 26: 220–221. [PubMed: 8599014]
57. Birch NC, Radio S, and Horslen S. 2003. Metastatic hepatocellular carcinoma in a patient with niemann-pick disease, type C. J Pediatr Gastroenterol Nutr 37: 624–626. [PubMed: 14581809]
58. Twarling A, Michael K, and Berg J. 2004. Sonographic evaluation of Niemann-Pick disease type C. J Diagn Med Sonogr 20: 198–201.
59. Beltroy EP, Richardson JA, Horton JD, Turley SD, and Dietschy JM. 2005. Cholesterol accumulation and liver cell death in mice with Niemann-Pick type C disease. Hepatology 42: 886–893. [PubMed: 16175610]
60. Praggastis M, Tortelli B, Zhang J, Fujiwara H, Sidhu R, Chacko A, Chen Z, Chung C, Lieberman AP, Sikora J, Davidson C, Walkley SU, Pipalia NH, Maxfield FR, Schaffer JE, and Ory DS. 2015. A murine Niemann-Pick C1 I1061T knock-in model recapitulates the pathological features of the most prevalent human disease allele. J Neurosci 35: 8091–8106. [PubMed: 26019327]
61. Vanier MT 2015. Complex lipid trafficking in Niemann-Pick disease type C. J Inherit Metab Dis 38: 187–199. [PubMed: 25425283]
62. Zampieri S, Mellon SH, Butters TD, Nevyjel M, Covey DF, Bembi B, and Dardis A. 2009. Oxidative stress in NPC1 deficient cells: protective effect of allopregnanolone. J Cell Mol Med 13: 3786–3796. [PubMed: 18774957]
63. Vazquez MC, del Pozo T, Robledo FA, Carrasco G, Pavez L, Olivares F, Gonzalez M, and Zanlungo S. 2011. Alteration of gene expression profile in Niemann-Pick type C mice correlates with tissue damage and oxidative stress. PLoS One 6: e28777. [PubMed: 22216111]
64. Fu R, Yanjanin NM, Bianconi S, Pavan WJ, and Porter FD. 2010. Oxidative stress in Niemann-Pick disease, type C. Mol Genet Metab 101: 214–218. [PubMed: 20667755]
65. Ishida Y, Nayak S, Mindell JA, and Grabe M. 2013. A model of lysosomal pH regulation. J Gen Physiol 141: 705–720. [PubMed: 23712550]
66. Liu B, Ramirez CM, Miller AM, Repa JJ, Turley SD, and Dietschy JM. 2010. Cyclodextrin overcomes the transport defect in nearly every organ of NPC1 mice leading to excretion of sequestered cholesterol as bile acid. J Lipid Res 51: 933–944. [PubMed: 19965601]
67. Tortelli B, Fujiwara H, Bagel JH, Zhang J, Sidhu R, Jiang X, Yanjanin NM, Shankar RK, Carillo-Carasco N, Heiss J, Ottinger E, Porter FD, Schaffer JE, Vite CH, and Ory DS. 2014. Cholesterol homeostatic responses provide biomarkers for monitoring treatment for the neurodegenerative disease Niemann-Pick C1 (NPC1). Hum Mol Genet 23: 6022–6033. [PubMed: 24964810]
68. Hoque S, Kondo Y, Sakata N, Yamada Y, Fukaura M, Higashi T, Motoyama K, Arima H, Higaki K, Hayashi A, Komiya T, Ishitsuka Y, and Irie T. 2020. Differential Effects of 2-Hydroxypropyl-Cyclodextrins on Lipid Accumulation in Npc1-Null Cells. Int J Mol Sci 21.

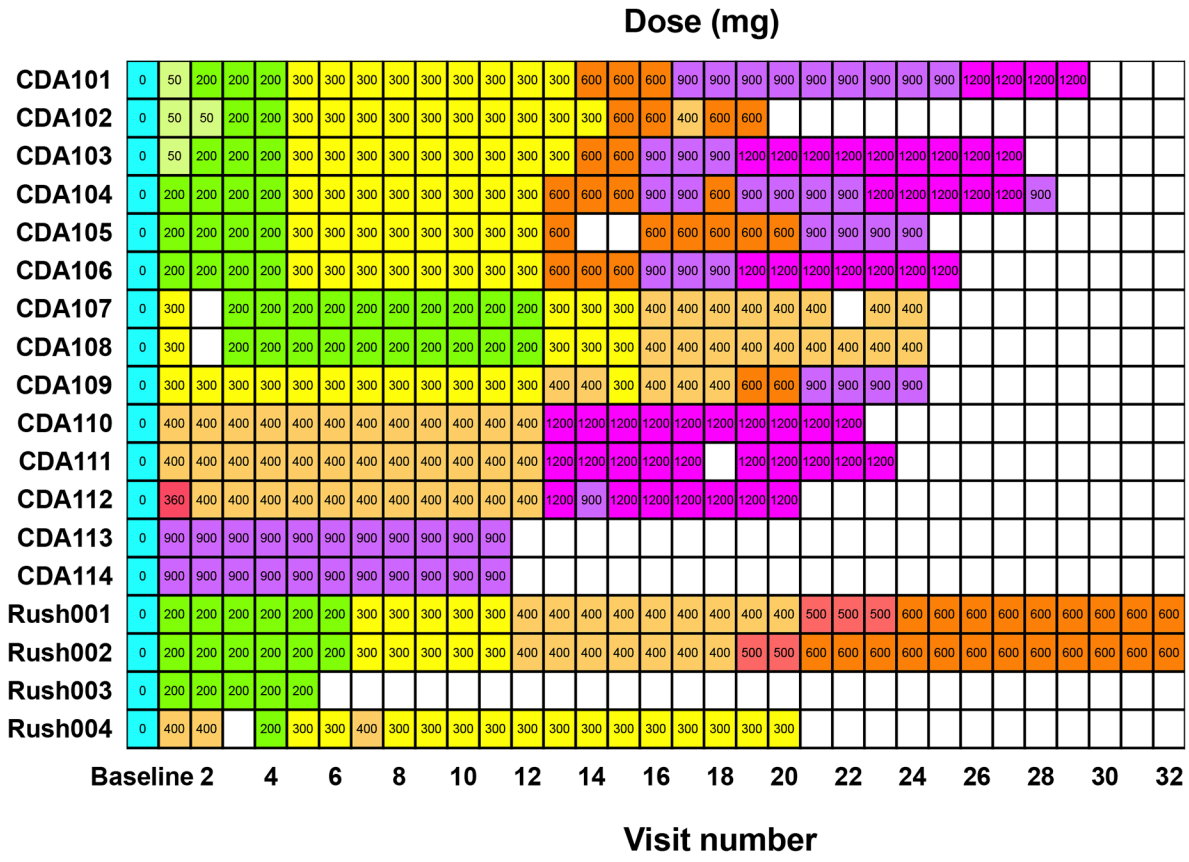

Figure 1.

HPBCD dosing for participants visited NIH and RUMC. The participants CDA101 – 114 received monthly doses at NIH, and the participants Rush001 – 004 received biweekly doses at RUMC. The treatment visits with missed doses are shown in the blank cells, and no plasma samples were drawn.

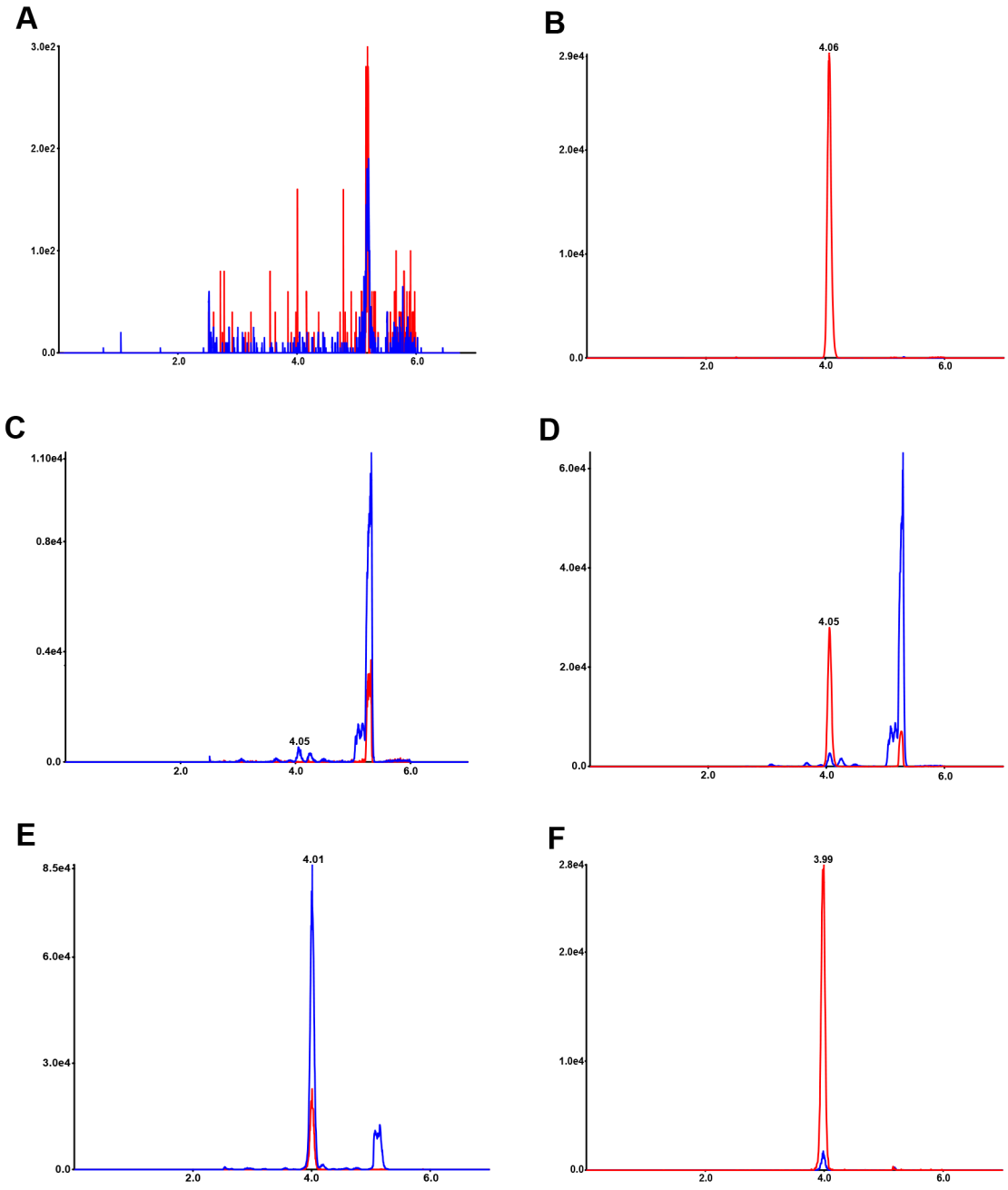

Figure 2.

LC-MS/MS chromatograms for TCG. Chromatograms of TCG and internal standard in blank (A), internal standard in blank (B), TCG in control plasma without internal standard (C), TCG in control plasma with internal standard (D), TCG in NPC1 plasma with internal standard (E), and TCG in LLOQ (F). TCG (m/z 464→74) are shown in blue and internal standards (m/z 467→77) in red, and their retention times are 4.0 min.

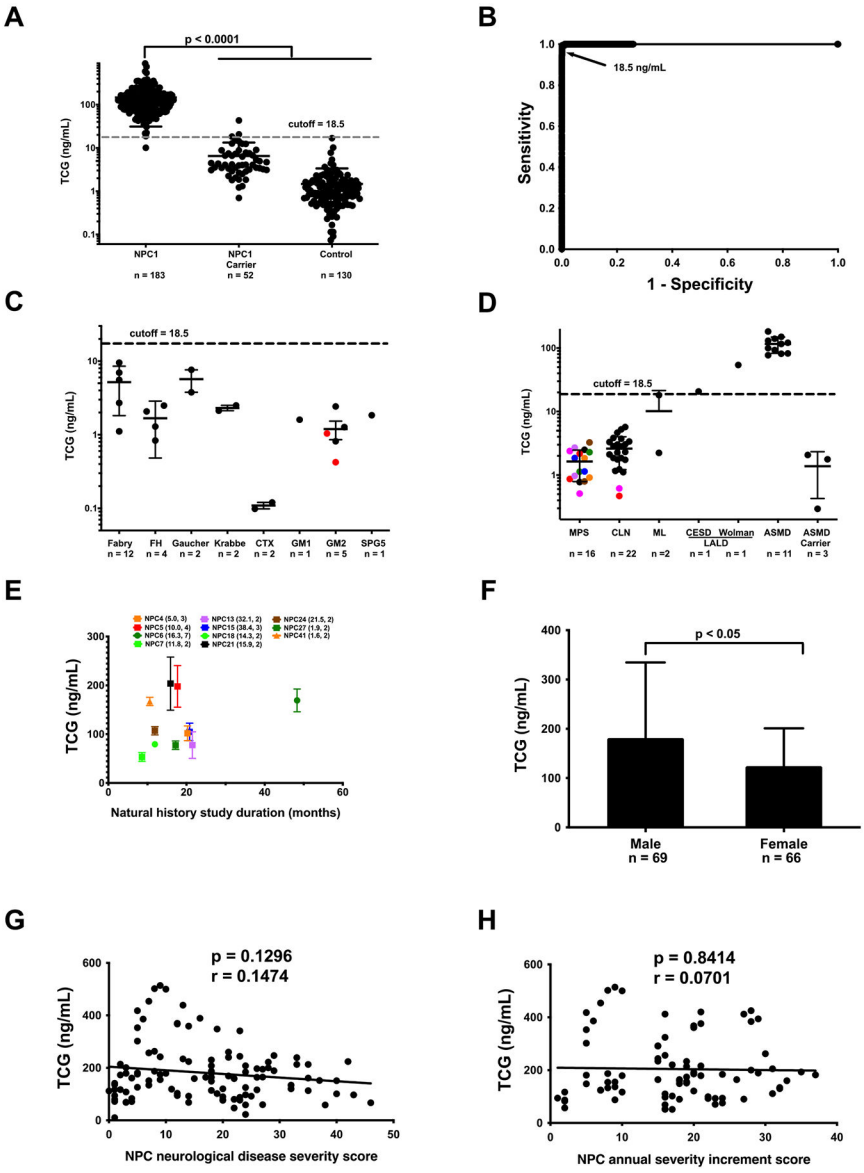

Figure 3.

Plasma TCG in patients affected with genetic diseases. (A) TCG in plasma samples from NPC1 affected (n = 183), NPC1 heterozygous (n = 53), and control (n = 130) subjects. Data are presented as mean ± standard deviation (SD). P < 0.0001 for NPC1 versus for heterozygotes and controls. (B) ROC curve demonstrates 0.9999 area under the curve for TCG. A cut-off value of 18.5 ng/mL yields a sensitivity of 0.9945 and specificity of 0.9982 to discriminate NPC1 affected individuals from controls and NPC1 heterozygotes. (C) TCG in plasma samples from patients with Fabry (n = 12), FH (n = 4), Gaucher (n = 2), Krabbe (n = 2), CTX (n = 2), GM1 (n = 1), GM2 including Tay-Sachs (black, n = 3) and Sandhoff (red, n = 2) diseases, and SPG5 (n = 1). Data are presented as mean ± SD. (D) TCG in plasma samples from patients with MPS I (black, n = 2), II (brown, n = 2), IIIA (orange, n = 2), IIIB (red, n = 2), IIIC (green, n = 2), IVA (pink, n = 2), VI (purple, n =2), VII (blue, n =2), Batten (CLN1, red, n = 1; CLN2, pink, n = 1; CNL3, black, n = 20), MLII/III (n = 2), CESD (n =

1), Wolman (n = 1), ASMD (n = 11) diseases, and ASMD carriers (n = 3). Data are presented as mean ± SD. (E) TCG in the plasmas collected from the NPC1 natural history study. The plasma samples were collected during 9 – 53 months study period. Data are presented as mean ± SD for each subject over the length of time in the natural history study. The age at enrollment (years) and number of samples collected during the study are given in parentheses. (F) Comparison of plasma TCG levels in male (n = 69) and female (n = 66) NPC1 patients. Data are presented as mean ± SD. $P < 0.05$ for male versus female. (G) Correlation of plasma TCG levels with NPC neurological disease severity scores. (H) Correlation of plasma TCG levels with NPC annual severity increment scores.

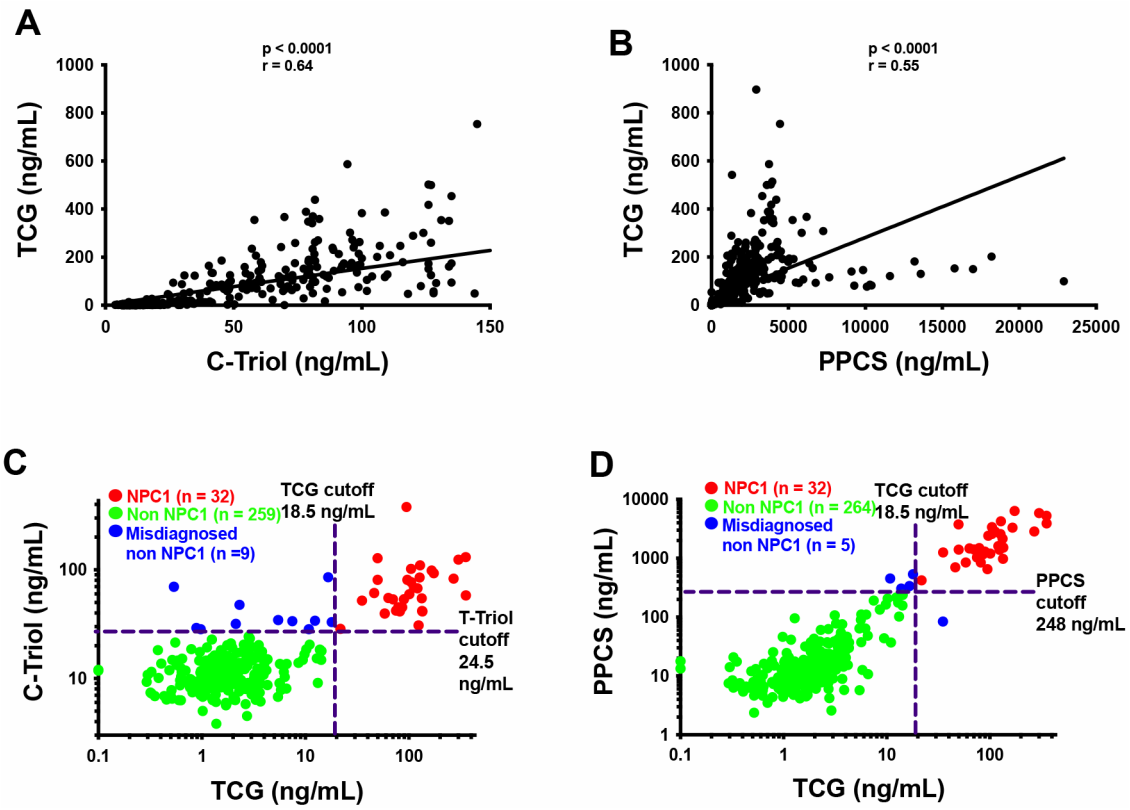

Figure 4.

Application of TCG and other NPC1 biomarkers to diagnose NPC1. (A) Correlation of plasma TCG levels with C-triol levels. (B) Correlation of plasma TCG levels with PPCS levels. (C) Comparison of diagnosis of NPC1 from unknown patients with TCG and C-triol. (D) Comparison of diagnosis of NPC1 from unknown patients with TCG and PPCS. The patient population are same in (C) and (D) except for the patient that was misdiagnosed by TCG, and this patient was diagnosed with PPCS and TCG only. TCG/C-triol (C) and TCG/PPCS levels (D) of each patient are plotted, and the patient was diagnosed as NPC1 when the biomarker was above the cutoff. The true NPC1, misdiagnosed non-NPC1, non-NPC1 are shown in red, blue, and green, respectively.

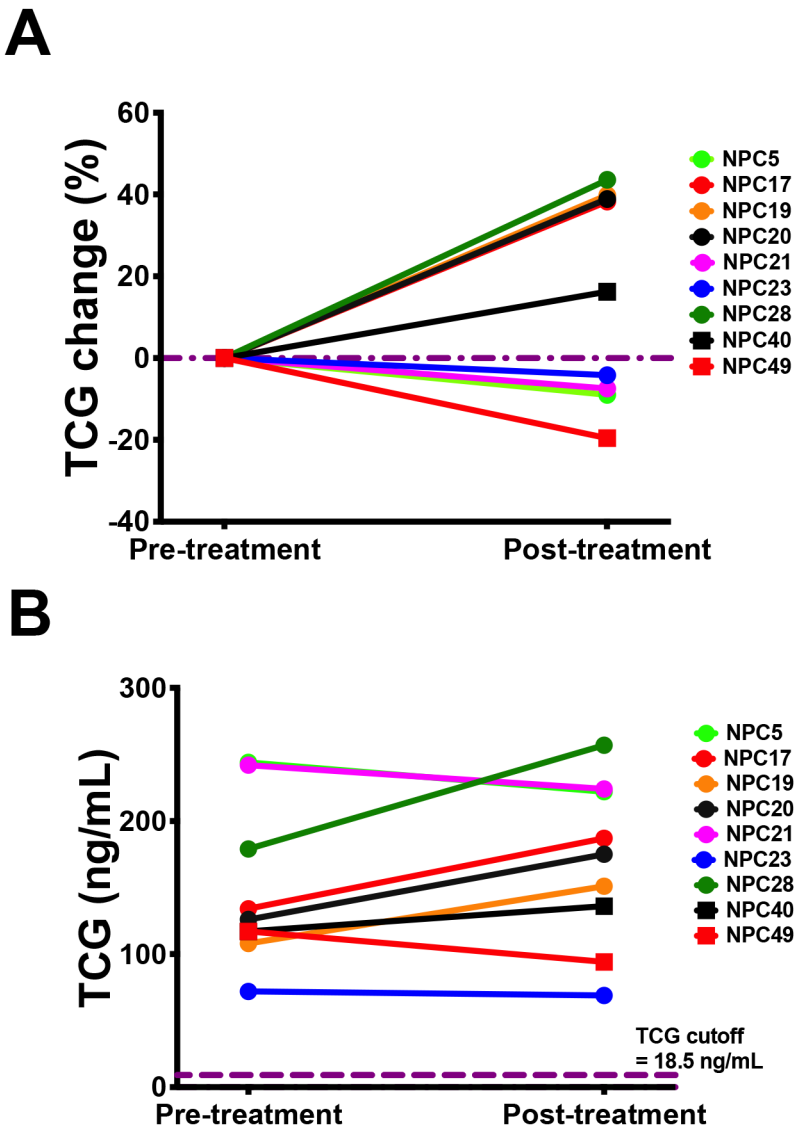

Figure 5.

Response of plasma TCG levels to miglustat treatment in NPC1 study participants. (A) Data are presented as percentage change of plasma TCG levels in post-treatment versus pre-treatment. $P > 0.05$ no significant. (B) TCG concentration in plasma samples collected from NPC1 study participants at pre- and post-treatments.

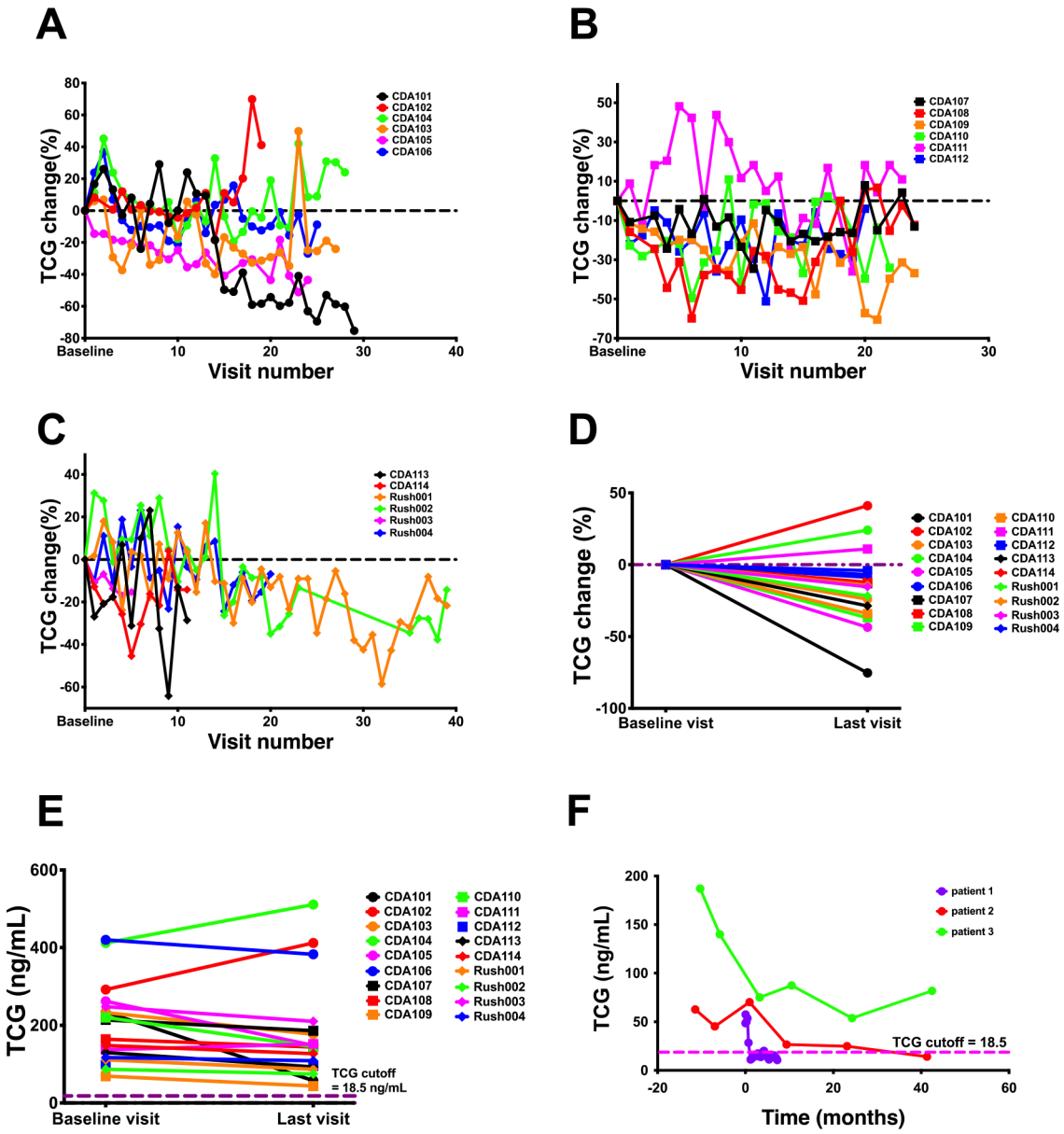

Figure 6.

Response of plasma TCG levels to HPβCD treatment in NPC1 study participants. (A - C) Percentage change of plasma TCG in NPC1 study participants receiving IT HPβCD treatment at each treatment visit versus baseline visit. The samples from Rush002 were not collected at visits 24 - 34. (D) Percentage change of plasma TCG in NPC1 study participants receiving IT HPβCD treatment at the last visit versus baseline visit. $P < 0.05$ for average of 15% decrease of TCG. (E) Plasma TCG concentrations in NPC1 study participants at the baseline and last visits of IT HPβCD treatment. (F) Response of plasma TCG concentration to weekly IV HPβCD treatment. The pre-treatment, treatment, and post-treatment time points are shown at negative, 0, and positive months, respectively.

Table 1.

Accuracy and precision statistics for TCG in human plasma

Run ID	QC Level	LLOQ	LLQC	LQC	MQC	HQC	DQC
	Nominal concentration	**1**	**1.65**	**11.7**	**402**	**802**	**1600**
1	Intra-run mean	0.97	1.64	12.22	405.67	786.33	1590.00
	Intra-run SD	0.0640	0.0735	0.6432	10.0731	12.6912	43.5890
	Intra-run %CV	6.59	4.48	5.26	2.48	1.61	2.74
	Intra-run %RE	−2.82	−0.61	4.42	0.91	−1.95	−0.63
	n	6	6	6	6	6	3
2	Intra-run mean	0.95	1.72	12.02	397.67	783.33	
	Intra-run SD	0.0541	0.0485	0.2137	8.5479	13.4263	
	Intra-run %CV	5.69	2.83	1.78	2.15	1.71	
	Intra-run %RE	−4.98	3.94	2.71	−1.08	−2.33	
	n	6	6	6	6	6	
3	Intra-run mean	0.97	1.74	12.12	397.00	781.33	
	Intra-run SD	0.0747	0.0983	0.3869	7.0143	13.0792	
	Intra-run %CV	7.72	5.67	3.19	1.77	1.67	
	Intra-run %RE	−3.23	5.15	3.56	−1.24	−2.58	
	n	6	6	6	6	6	
Inter-run mean		0.96	1.68	12.12	400.11	783.67	
Inter-run SD		0.0616	0.0845	0.4315	9.0676	12.4570	
Inter-run %CV		6.40	5.02	3.56	2.27	1.59	
Inter-run %RE		−3.68	1.97	3.56	−0.47	−2.29	
n		18	18	18	18	18	